

## Design of Elastomeric Bearing System and Analysis of its Mechanical Properties

**Byung-Young Moon\***, **Gyung-Ju Kang**, **Beom-Soo Kang**  
*Department of Aerospace Engineering, Pusan National University,  
Gumjung-ku, Busan 609-735, Korea*

**Dae-Seung Cho**

*Department of Naval Architecture and Ocean Engineering, Pusan National University, Korea*

This paper proposes a new type of bearing system. In this study, a method for design of an elastomeric bearing system and its mechanical property analysis are carried. Experimental and theoretical studies of the elastomeric bearings with fiber reinforcement were proved effective new lightweight bearing system. The fibers in the bearings for isolation are assumed to be flexible in extension, in contrast to the steel plates in the conventional bearing system. Several kinds of bearing systems in the form of long strips are designed, fabricated and tested. The results suggest that it is possible to produce the economical and effective fiber-reinforced elastomeric bearing that matches the behavior of a steel-reinforced bearing. Feasibility and advantages of the proposed bearings are illustrated by the application of the analytic procedure to the structure system. Results obtained here are reported to be an efficient approach with respect to bearing system and design of bearing against shock absorbing system when compared with other conventional one.

**Key Words :** Shock Absorbing System, Design of Elastomeric Bearing, Modeling of Bearing System, Stiffness Analysis, Shock Excitation, Energy Dissipation System

### 1. Introduction

As a shock absorbing system, a base isolation technique has played a key role in passive seismic protective systems. This system has emerged as a viable structural option in seismic zones to reduce the vulnerability of structural systems subjected to earthquakes, such as computer center, chip fabrication factories and hospital. The importance of the base isolation design is recognized to protect structures from the strong earthquakes after 1994 Northridge earthquake and researchers have considerable attention (Koo, 1998 ;

Koo, 1999). The rubber bearing is the most popular type of base isolation and it can be made very stiff in the vertical direction to take the vertical load, and very flexible in the horizontal direction to isolate the horizontal vibrations. The main aim of this system is to shift the natural frequencies of structures to a lower value, to avoid structural resonance. Base isolation has been an attractive solution and has found many practical applications.

However, recent earthquakes in India, Turkey and South America made major loss of life. Especially the disaster is worse when the earthquake occurs in developing country. Even in relatively moderate earthquakes in areas with poor housing many people are killed by the collapse of brittle heavy unreinforced masonry or poorly constructed concrete buildings. Even though there is seismic elastomeric bearing to prevent these losses, seismic isolators currently used are heavy and

---

\* Corresponding Author,

**E-mail :** moonby20@hanmail.net

**TEL :** +82-51-510-1531; **FAX :** +82-51-510-3760

Department of Aerospace Engineering, Pusan National University, Gumjung-ku, Busan 609-735, Korea.  
(Manuscript Received August 9, 2002; Revised November 15, 2003)

expensive to apply to low-cost house. The conventional seismic isolators consist of rubber and steel layers. Because steel plates are used for the reinforcement, the manufacturing process of isolator is complicate. Hence, the steel reinforced isolator becomes heavy and expensive. The role of steel plates in the isolator is to maintain vertical load from the building. In order to reduce the weight of the isolator, the reinforcement can be replaced by other material, which is lighter than steel and high in tensional stiffness.

If the reinforce is replaced with fiber, fiber reinforced elastomeric isolator could sustain vertical stiffness and reduce weight. However, the study, which applied the fiber reinforced system to the design of elastomeric bearing, has not been reported yet. Authors reported studies, which were conducted on circular type isolator with multi-layer of fiber plate and rubber plate between top and bottom steel plates (Moon 2002 ; Moon 2002).

However, in this paper the strip type fiber reinforced elastomeric isolator consisting of the multi-layer of fiber and rubber plate is suggested.

Therefore, this paper presents an analytical technique based on the theory and experiment for the new bearing systems, which focuses on the mechanical properties of the proposed strip type isolator. The realization of the idea that strip type isolator is easy to cut to desired size is also considered. Experimental tests for the evaluation of mechanical properties were carried out on the fabricated strip-type fiber reinforced isolators.

The theoretical approaches of vertical stiffness of fiber and rubber layer are suggested on the base of compression theory for rubber and rigid reinforced elastomeric isolator. The fiber reinforced elastomeric isolator was fabricated with the same dimensions of conventional isolator and experimental test was carried out. The result showed that fiber could be used in elastomeric isolator.

## 2. Design of Strip Type Isolators

A conventional isolator consists of rubber layer and steel plates, as shown in Fig. 1. The role of

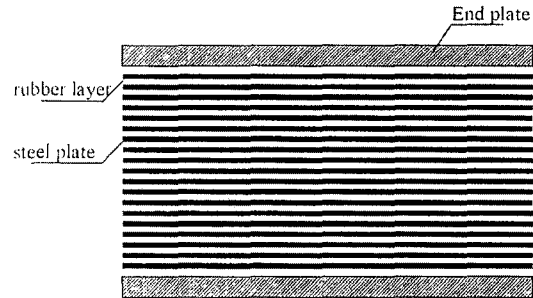


Fig. 1 Model of steel reinforced elastomeric isolator

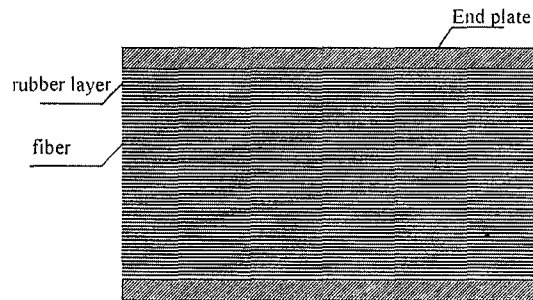


Fig. 2 Model of fiber reinforced elastomeric isolator

steel plate in the isolator is sustaining the vertical load of upper structure. Because of the weight of the steel plate, total weight of a isolator becomes heavy. In order to reduce the total weight of a isolator, the steel reinforce has to be replaced by other material lighter than steel and stiff enough to sustain the vertical loads. As a reinforcement in the isolator fibers can be used, which satisfy the previous conditions. Fig. 2 shows section model of fiber reinforced elastomeric isolator of circular type, which consists of rubber layer and fiber reinforce. Long strip type isolators could be designed and easily cut to required size.

### 2.1 Compression of pad with rigid reinforcement

The vertical stiffness of a rubber bearing is given by the formula

$$K_v = \frac{E_c A}{t_r} \quad (1)$$

where  $A$  is the area of the bearing,  $t_r$  is the total thickness of rubber, and  $E_c$  is the instantaneous compression modulus of the rubber-steel composite under the specified level of vertical load. The

value of  $E_c$  for a single rubber layer is controlled by the shape factor,  $S$ , defined as

$$S = \frac{\text{loaded area}}{\text{free area}} \quad (2)$$

Fig. 3 shows the infinitely long rectangular pad with rigid reinforce, which consist of rubber layer with width of  $2b$  and a thickness of  $t$  and rigid plates. The compression modulus becomes

$$E_c = \frac{B}{A \varepsilon_c} \quad (3)$$

where  $P$  is resultant normal load,  $\varepsilon_c = \Delta/t$  is compression strain, where the change of thickness of the pad is  $\Delta$ . Since the shape factor of infinite strip of width  $2b$  is  $S = b/t$ , and the area per unit length is  $A = 2b$ ,

$$E_c = 4GS^2 \quad (4)$$

where  $G$  is shear modulus of rubber.

This is the effective compressive modulus of an infinitely long strip layer of elastomer bonded to the rigid reinforcement (Kelly, 1999).

## 2.2 Compression stiffness with flexible reinforcement

The rigid reinforce on the top and bottom plates in Fig. 3 is replaced by flexible reinforce

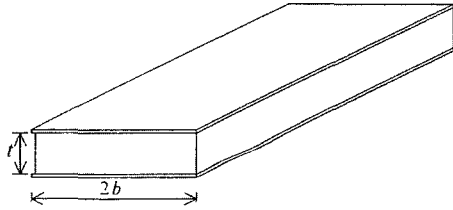


Fig. 3 Infinitely long rectangular pad

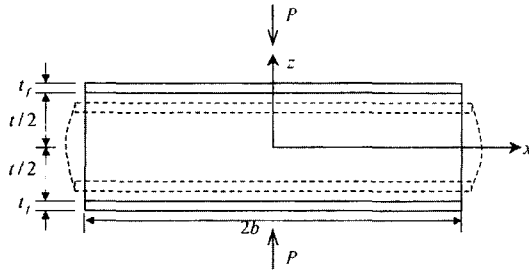


Fig. 4 Fiber reinforced infinitely long strip layer

as shown in Fig. 4. The top and bottom surfaces of the layer are perfectly bonded to flexible reinforces that are modeled as an equivalent sheet with a thickness of  $t_f$  and the isolator is under compression load  $P$ .

For the shape factor is large (say  $>20$ ), the estimate of  $E_c$  becomes comparable to the value of the bulk modulus of the material. The bulk modulus of natural rubber is approximately 2000 Mpa and in this case neglecting compressibility is not justified. To include the influence of compressibility on the behavior of a pad in compression, compressibility equation becomes

$$\varepsilon_{xx} + \varepsilon_{zz} = -\frac{p}{K} \quad (5)$$

where  $\varepsilon_{xx}$ ,  $\varepsilon_{zz}$  is component strain of  $x$ ,  $z$  respectively and  $K$  is the bulk modulus.

The effective compression modulus becomes (Kelly, 2002)

$$E_c = K \frac{\lambda}{\lambda + \mu} \left( 1 - \frac{\tanh(\lambda + \mu)^{\frac{1}{2}}}{(\lambda + \mu)^{\frac{1}{2}}} \right) \quad (6)$$

where  $\lambda = \frac{12Gb^2}{Kt^2}$ ,  $\mu = \frac{12Gb^2}{E_f t_f t}$ , and  $E_f$  is elastic modulus of the reinforcement.

The compression modulus of flexible reinforce is compared with compression modulus of rigid reinforce in Fig. 5. It explains how the compression modulus decreases with increasing flexibility. Compression modulus of rigid reinforce becomes  $E_c = 4GS^2$  as the Eq. (4) and  $E_c/GS^2$  becomes four, when  $ab$  is zero, where  $a = (\lambda)^{1/2}$ .

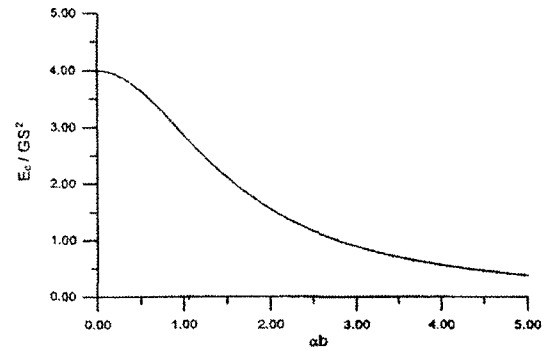
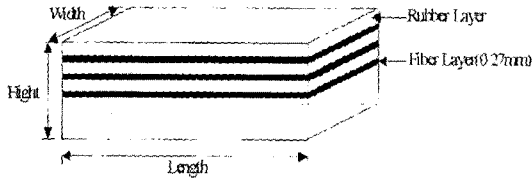


Fig. 5 Normalized effective compression modulus as a function of  $ab$

**2.3 Bending stiffness of a single pad**

The response of a single pad to an applied bending moment is also an important aspect of isolation bearings, since the bending stiffness of a pad plays an important role in providing the resistance of the whole bearing to buckling under a compressive load. In the case of the strip isolator the buckling is in the short direction and the buckling problem is complicated in the case of the unbounded bearings by the fact that the boundary conditions involve a possible uplift. Nevertheless an adequate bending stiffness is essential to prevent lateral instability. In Fig. 7, a deformation is visualized. The moment,  $M$ , is given by



**Fig. 6** Model of strip type fiber reinforced elastomeric isolator

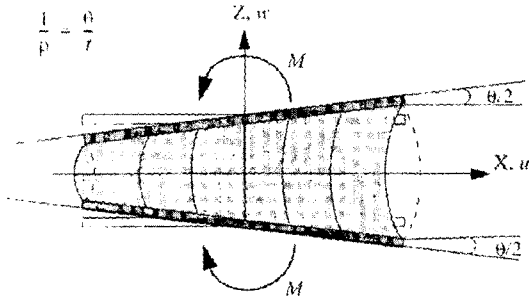


**Fig. 7** Pad in Pure flexure

$$M = \frac{E_f^2 t_f^2}{6Gt} \theta b \left( 1 + \frac{\alpha^2}{3} - \frac{\alpha}{\tanh \alpha} \right) \quad (7)$$

Here,  $\theta$  is the angle between the rigid plates in the deformed configuration and the bending about the y-axis.

Eq. (7) gives for the effective bending stiffness

$$(EI)_{eff} = \frac{M}{\theta/t} = \frac{E_f^2 t_f^2 b}{6G} \left( 1 + \frac{\alpha^2}{3} - \frac{\alpha}{\tanh \alpha} \right) \quad (8)$$

**3. Experimental Test**

**3.1 Experimental test model of strip type isolator**

Several samples of fiber reinforced strip type isolators, as shown in Fig. 6, were designed, fabricated and tested in compression and shear to verify whether the approach was practical or not. Seven specimens were tabulated in the type of strips with slightly different geometric dimensions as given in Table 1.

In order to reach a desired level of vertical pressure within the capacity of the testing machine, two of the strips were cut in half and these halves were used as test specimens. The total thickness of rubber in each bearing was 99 mm, and they were reinforced by 30 plane sheets of 0.27 mm thick carbon fiber. The experimental observation was carried out to study the behavior of the fiber-reinforced strips in compression and in shear at various levels of vertical pre-load. The average vertical stiffness of the bearing was obtained from a compression test in the following way. The specimen was monotonically loaded up to the target value of vertical pressure and then

**Table 1** Test specimens

Name	Length [mm]	Width [mm]	Height [mm]	Area [mm <sup>2</sup> ]	Comments	Presence of rubber cover			
						East	West	North	South
DRB1	735	183	105	134505		Yes	No	No	No
DRB2	750	190	105	142500		Yes	No	Yes	No
DRB3	740	190	105	140600		No	Yes	Yes	No
DRB4	365	190	105	69350	Cut from 190×755×105	No	No	Yes	No
DRB5	390	190	105	74100	Cut from 190×755×105	Yes	No	Yes	No
DRB6	377	183	105	68991	Cut from 183×755×105	No	Yes	No	No
DRB7	377	183	105	68991	Cut from 183×755×105	No	No	No	No

three cycles of vertical loading with small amplitude about this target value were performed. The shear stiffness of the specimens was obtained from a shear test, in which sets of shear cycles with step-wise increasing amplitude were applied. These shear test values of vertical pressure and then three cycles of vertical loading with small amplitude about this target value were performed. The shear tests were carried out for various values of vertical pressure and for three angles between the testing direction and the longitudinal direction of the strip: 0 degree, 90 degree, and 45 degree. Vertical test results for DRB1 with 1.73 MPa vertical pressures are presented in Fig. 8(a) and 3.45 MPa vertical pressures are presented in Fig. 8(b). The results show that the average stiffness of DRB1 is 550 MN/m in Fig. 8(a) and 791 MN/m in Fig. 8(b).

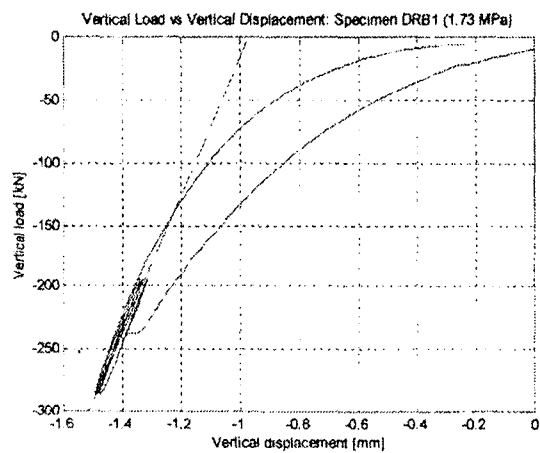
### 3.2 In-plane test machine

The test machine was designed to carry out in-plane vertical and horizontal cyclic loading tests. The vertical load was applied to the specimen by two 570 kN hydraulic actuators, through a stiff frame. The horizontal load was applied to the same frame by a 450 kN hydraulic actuator. The test machine had a displacement capacity of  $\pm 254$  mm in the horizontal direction and a load capacity of  $\pm 1,140$  kN in the vertical direction. Two sets of tests were carried out. The vertical test was carried out using a vertical load control, and the horizontal test was performed using a horizontal displacement control.

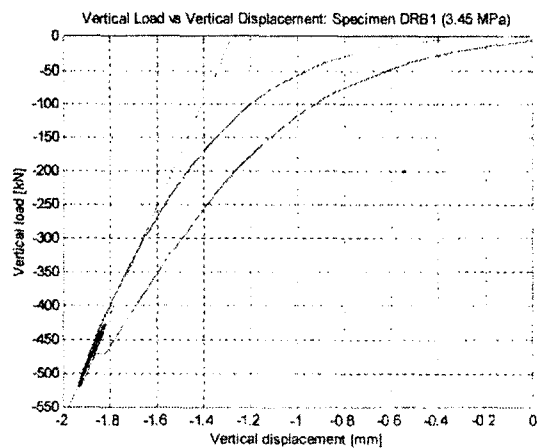
### 3.3 Test instrumentation and loading history

Many sensors were used to monitor the response of the specimen during the test in order to understand the specimen behavior. The instrumentation allocation was slightly different for the vertical and horizontal tests. The loading history is varied from test to test. The specimen DRB1 was tested under vertical load control during the vertical test. The specimen was monotonically loaded to 1.73 MPa of vertical pressure and three fully reversed cycles with  $\pm 0.35$  MPa amplitude were performed. In the final stage of the vertical test the specimen was monotonically unloaded. The similar test at 3.45 MPa original vertical pressures with  $\pm 0.35$  MPa amplitude was performed also to study the vertical stiffness at higher values of vertical load. The horizontal test was performed under horizontal displacement control. The

specimen DRB1 was tested in cyclic shear, with three fully reversed cycles at four maximum strain levels of 25%, 50%, 75%, and 100% (based on 99 mm rubber thickness). Three cycles were applied at a vertical pressure of 1.73 MPa. The value of the vertical pressure was increased to 3.45 MPa and the same shear test was performed. Shear test was carried out for the following sequence of the angle between the testing direction and the longitudinal direction of the strip: 0 degree, 90 degree, and 45 degree. Vertical test results for DRB1 with 1.73 MPa vertical pressures are presented in Fig. 8(a) and 3.45 MPa vertical pressures are presented in Fig. 8(b). The results show that the average stiffness of DRB1 is 550 MN/m in Fig. 8(a) and 791 MN/m in Fig. 8(b).

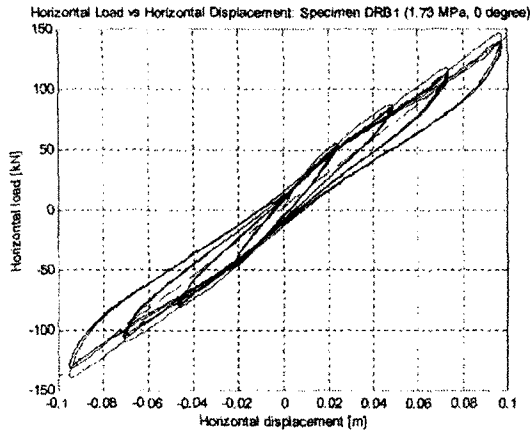


(a) 1.73 MPa vertical pressure

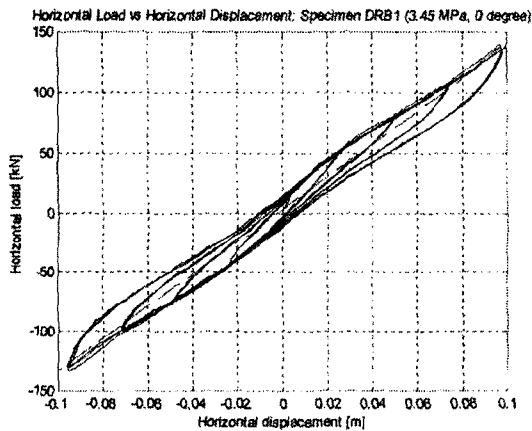


(b) 3.45 MPa vertical pressure

Fig. 8 Vertical test results for DRB1



(a) With 1.73 MPa vertical pressure (0 degree)

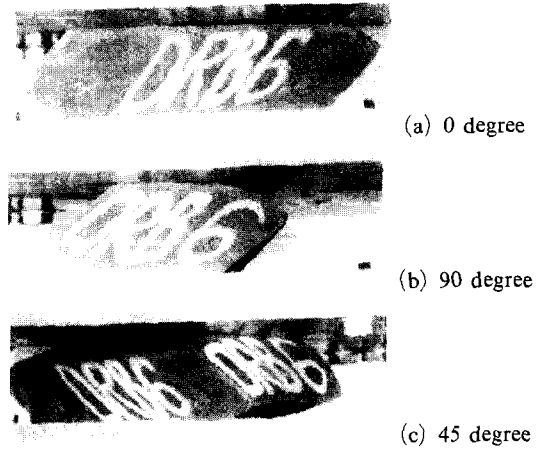


(b) 3.45 MPa vertical pressure (0 degree)

**Fig. 9** Horizontal test results for DRB1

The average stiffness increases with increase of vertical load. It shows that the isolator has an ability to sustain the vertical load. Horizontal test results for DRB1 with 1.73 MPa vertical pressures (0 degree) have shown in Fig. 9(a) and 3.45 MPa vertical pressures (0 degree) has shown in Fig. 9 (b). The average stiffness is 1408.6 kN/m under 1.73 MPa vertical pressures, and 1354.3 kN/m under 3.45 MPa vertical pressures, it makes differences within 5%. It shows that the isolator has steady conductivity from vertical load.

Specimens DRB2 and DRB3 were tested under the same test program, but with different sequence of the angle between the testing direction and the longitudinal direction of the strip. The sequence of the angle for specimen DRB2 is 45 degree, 0 degree, and 90 degree. The sequence of the angle

**Fig. 10** Specimen DRB6 at 100% shear deformation

for specimen DRB3 is 90 degree, 45 degree, and 0 degree.

To show an example of global behavior of the specimens during these tests the images of specimen DRB6 under deformation are included.

A photo of the specimen under 100% shear deformation testing in the longitudinal direction is presented in Fig. 10(a). At 0 degree longitudinal direction of isolator and loading direction is concurrent. Even at 100% shear deformation top and bottom plates of test machine are contacted closely with isolator, and it shows stable deformation. On the other hand, at 90 degree shear deformation, the area which contacts test machine and isolator is narrow, hence there is a concentration of load. There must be a reduction of seismic isolation ability in 90 degree direction. Fig. 10(b) is a photo of the specimen DRB6 under 100% shear deformation testing at 90 degree to the longitudinal direction. The view of the deformation with the same magnitude at 45 degree to the longitudinal direction is presented in Fig. 10(c). At 45 degree deformation shape shows an average between 0 degree and 90 degree.

## 4. Discussion of Experimental Results

### 4.1 Horizontal test results

The shear modulus ( $G$ ) of this natural rubber compound is 0.690 MPa. The three full-length

uncut specimens had an average area ( $A$ ) of  $0.140 \text{ m}^2$  and a total rubber thickness ( $t_r$ ) of  $0.099 \text{ m}$ . The horizontal stiffness,  $K_H$ , of a conventional isolator is given by

$$K_H = GA/t_r \quad (9)$$

and for these values  $K_H$  is  $970 \text{ kN/m}$ .

At 100% shear strain and a pressure of  $1.73 \text{ MPa}$  the average horizontal stiffness in the longitudinal loading direction is  $1280 \text{ kN/m}$ , in the lateral loading direction is  $863 \text{ kN/m}$  and at  $45^\circ$  is  $1120 \text{ kN/m}$ . It is clear that the horizontal stiffness of fiber-reinforced isolator in  $0$  degree and  $45$  degree direction is superior to conventional isolator.

The hysteresis loops for the longitudinal loading direction tend to stiffen when the shear strain is increased from 100% to 150% whereas for the lateral loaded direction the loops turn over so that the instantaneous tangent stiffness is negative at the larger strains. However the effect is reduced at higher-pressure levels. The  $45^\circ$  loading does not produce either stiffening or softening but gives values intermediate between the  $0^\circ$  and  $90^\circ$  loadings.

The value of the stiffness at 100% shear strain in the longitudinal direction is slightly higher than would be expected from the nominal value of the shear modulus but in the transversal loading direction the stiffness is lower. At  $45^\circ$  the stiffness is intermediate between the other two. If we assume that the layout of the strip isolator is orthogonal with roughly the same number in each direction the average between  $0^\circ$  and  $90^\circ$  is close to the value at  $45^\circ$  so that the system will have the same period in any direction of movement.

The period can be roughly estimated using the pressure ( $p$ ) and the effective shear modulus. The period  $T$  is given by

$$T = 2\pi \sqrt{\frac{pt_r}{Gg}} \quad (10)$$

where  $g$  is gravity constant. If the average pressure over the system is  $3.45 \text{ MPa}$  as in the tests and the modulus ( $G$ ) is  $0.690 \text{ MPa}$  with  $99 \text{ mm}$  of rubber, then a period is  $1.4$  seconds. From the code formula this would produce a displacement

of  $143 \text{ mm}$  and a shear strain ( $\gamma$ ) of  $1.41$ , where shear strain ( $\gamma$ ) is ratio of maximum displacement to total rubber thickness. Adjusting the values to correspond to the measured stiffness at  $\gamma=1.5$ , we find that the period increases to  $1.5$  seconds and the displacement to  $150 \text{ mm}$ . This value satisfies the current UBC code for seismic isolation (Int. Conf. of Building Officials 1997) formulation that minimum isolation displacement would be around  $15 \text{ cm}$  for a  $1.5$  second system.

This suggests that if the period of  $1.5$  seconds is acceptable as the target value for the design of the building, the tested strip isolators would be adequate in the case that the average pressure could be at least  $3.45 \text{ MPa}$ . A longer period can be obtained by laying one isolator on top of another. This leads a periodical objectives possible. If it is necessary to have an average pressure of less than  $3.45 \text{ MPa}$ , it is possible to use a softer compound. Compounds with shear moduli, at 100% strain, down to  $0.40 \text{ MPa}$  are available.

#### 4.2 Vertical test results

The vertical test results are shown in Tables 2, 3 and 4. Since the dimensions of the bearings are slightly different in each case. It is useful to tabulate the vertical stiffness in terms of the effective compression modulus as defined by Eq. (3). The first point to note is that there is a considerable variation in this value. The full-length bearings DRB1, DRB2 and DRB3 are quite consistent at around  $414 \text{ MN/m}^2$ . The two sets of half-length bearings have consistently lower values of  $E_c$  at the same vertical pressures of testing. The pair denoted by DRB6, DRB7 were tested at  $0.87 \text{ MPa}$ ,  $1.73 \text{ MPa}$  and  $3.45 \text{ MPa}$ . At the common test pressure of  $3.45 \text{ MPa}$ , the average of the two values of  $E_c$  was the same at the same vertical pressure of test.

The pair denoted by DRB4, DRB5 were not tested at  $1.73 \text{ MPa}$  but at  $3.45 \text{ MPa}$ , and  $6.90 \text{ MPa}$  tested. The set denoted by DRB6, DRB7 were tested at  $0.87 \text{ MPa}$ ,  $1.73 \text{ MPa}$  and  $3.45 \text{ MPa}$ . At the common test pressure of  $3.45 \text{ MPa}$ , the average of the two values of  $E_c$  of DRB4, DRB5 was the same as that of DRB6, DRB7 so that we can interpret the effect of variation of the target

**Table 2** Vertical test results for 1.73 Mpa vertical pressure

Specimen No.	Area [m <sup>2</sup> ]	Imposed Load [kN]	Average Pressure [MPa]	Average Stiffness $K_{av}$ [kN/m]	Compression Modulus $E_c$ [MPa]
DRB1	0.135	233.6	1.73	550853.9	404
DRB2	0.143	233.6	1.63	602975.0	417
DRB3	0.141	233.6	1.66	597053.3	419
DRB4	0.069	N/A	N/A	N/A	N/A
DRB5	0.074	N/A	N/A	N/A	N/A
DRB6	0.069	120.2	1.74	251687.8	361
DRB7	0.069	120.2	1.74	278983.5	400

**Table 3** Vertical test results for 3.45 Mpa vertical pressure

Specimen No.	Area [m <sup>2</sup> ]	Imposed Load [kN]	Average Pressure [MPa]	Average Stiffness $K_{av}$ [kN/m]	Compression Modulus $E_c$ [MPa]
DRB1	0.135	467.3	3.46	791048.8	580
DRB2	0.143	467.3	3.27	849319.3	588
DRB3	0.141	467.3	3.31	752785.8	529
DRB4	0.069	253.7	3.68	349938.19	502
DRB5	0.074	253.7	3.43	352040.6	471
DRB6	0.069	240.3	3.48	328721.9	472
DRB7	0.069	240.3	3.48	351392.3	504

**Table 4** Vertical test results for extreme values of vertical pressure

Specimen No.	Area [m <sup>2</sup> ]	Imposed Load [kN]	Average Pressure [MPa]	Average Stiffness $K_{av}$ [kN/m]	Compression Modulus $E_c$ [MPa]
DRB1	0.135	N/A	N/A	N/A	N/A
DRB2	0.143	N/A	N/A	N/A	N/A
DRB3	0.141	N/A	N/A	N/A	N/A
DRB4	0.069	507.3	7.35	467372.6	671
DRB5	0.074	507.3	6.86	445858.5	596
DRB6	0.069	60.1	0.87	175617.3	252
DRB7	0.069	60.1	0.87	167190.4	240

pressure over an eight-fold range of value. The fact that at the same pressure the  $E_c$  values for the full length bearings is higher than for the half length bearings is most likely to be due to the longer influence of free ends in the latter case. The theoretical analysis is developed for the infinite length strip and for the full-length bearings. The length to height ratio of 7.5 is large enough that this assumption is valid. At half of this value, the end effects can be expected to have

some influence. The vertical stiffness of an elastomeric isolation bearing is always difficult to measure since the displacements at the vertical loads corresponding to practical use are extremely small and a great deal of scatter is to be expected.

It is clear however that for all test specimens there is a systematic increase in stiffness and  $E_c$  when the central value of the pressure is doubled from 1.73 Mpa to 3.45 Mpa. As shown in Tables 2, 3 and 4, at the higher pressure the average



compression modulus of the first three full-length isolators increase to 565 Mpa from 413 MPa.

The half-length bearing tests show a systematic increase in  $E_c$  over the complete range of pressure. The increase is not linear in pressure but tends to decrease with increasing pressure from 55% at the lowest level to 15% at the highest. This is consistent with the type of carbon fiber used in the bearings. The fiber is woven, two directional and epoxied into a thin sheet. As the pressure increases, the in-plane fiber sheet tension increases and tends to straighten out the fiber strands, thus increasing the effective fiber modulus. To assess the effect of the various parameters on the vertical stiffness, it is necessary to estimate the actual shear modulus from the tests on shear. At a vertical pressure of 3.45 MPa the average shear stiffness of the first three bearings when tested in the longitudinal direction  $0^\circ$  is 1.278 MN/m which with an average area of  $0.140 \text{ m}^2$  and a thickness of rubber of 99 mm. This implies a shear modulus of 0.904 MPa, which is considerably larger than the nominal modulus from the fabricator. This use of the longitudinal tests to provide an estimate of the modulus is warranted by the fact that this case will have the least influence of the roll-off from the unbonded end condition. A steel reinforced isolator with this shear modulus, this area of rubber thickness would, if compressibility effects are ignored, have an effective compression modulus  $E_c$  given by Eq. (6), of  $3738 \text{ MN/m}^2$ . When compressibility is taken into account the effective modulus is considerably reduced as given by Eq. (10). To estimate  $E_c$  we use  $K=2000 \text{ Mpa}$  giving  $\lambda=5.3$ ,  $\mu=0$  and from Eq. (10) we have  $1150 \text{ MN/m}^2$ . The average measured value  $563 \text{ MN/m}^2$ , can be used to deduce the effect of the extensibility of the carbon fiber reinforcement. For this purpose we now turn to Eq. (10) and assume that  $\lambda=5.3$ . From the results we have  $E_c/K=0.28$  and from the equation we determine that  $(\lambda+\mu)^{\frac{1}{2}}=3.7$  implying  $\mu=8.39$ . When the known values of the various parameters are inserted into the definition of  $\mu$  we obtain finally the estimate of  $E_f$  as 14406 MPa.

It is certainly possible that the quality of the reinforcing could be improved but it is clear

**Table 5** Estimation of Effective bending stiffness of DRB1

Direction (degree)	Length (2b) (m)	b (m)	Effective bending stiffness (MN-m)
0	0.735	0.3675	2.324
90	0.183	0.0915	0.578

that this poor quality sheet is adequate for these bearings. An effective compression modulus  $E_c$  of  $563 \text{ MN/m}^2$  at an average pressure of 3.45 MPa implies a vertical vibration frequency of 20 Hz, which is more than necessary in any isolation application. From these results, the conclusion is that although the fiber is suspected to be very low quality, and presumably low-cost, it has sufficient strength for application to low-cost isolators.

### 4.3 Effective bending stiffness estimation

The value of  $E_f$  was estimated as 14406 Mpa and  $\alpha^2=\lambda$  was calculated as 5.3 in the previous section. The fiber thickness  $t_f$ , shear modulus of rubber  $G$  is 0.27 mm and 0.6901 Mpa, respectively. The effective bending stiffness can be estimated from the Eq. (8). For DRB 1, effective bending stiffness can be estimated. The estimation results are shown in Table 5.

## 5. Conclusions

In this paper, the strip type fiber reinforced elastomeric isolator is designed, fabricated and tested. To investigate the performance of the isolators, theoretical analysis and experimental tests are carried out. Theoretical approaches are provided for the analysis of the fiber reinforced strip isolators with several reasonable assumptions. From the horizontal test, the horizontal stiffness of fiber-reinforced isolator in 0 degree, and 45 degree of direction is superior to conventional isolator. Also it is shown that for a specified period system the isolator satisfied the current UBC code for seismic isolation formulation. From the vertical test at an average pressure level, an adequate vertical vibration frequency is obtained, which is more than necessary in any isolation application with effective compression

modulus.

The results reported herein will provide the better understanding of fiber reinforced bearing and the fact that the isolator can be made in long wide sheets and cut to the required width.

### Acknowledgment

This work was partially supported by Advanced ship Engineering Research Center of the Korea Science and Engineering Foundation.

### References

- Int. Conf. of Building Officials, 1997, Earthquake regulations for seismic isolated structures, Uniform Building Code, Appendix Chapter 16, Whittier, CA.
- Kelly, J. M., 2000, "Analysis for Fiber-Reinforced Elastomeric Isolators," *Annual Report to Engineering Research Center for Net-Shape and Die Manufacturing Pusan National University Korea*.
- Kelly, J. M., 1999, "Analysis of Fiber-Reinforced Elastomeric Isolators," *JSEE*, Vol. 2, No. 1, pp. 19~34.
- Kelly, J. M., 2002, "Analytical and Experimental Study on Fiber-Reinforced Strip Isolators," *Report to Dongil Rubber Belt company LTD*, p. 20.
- Koo, G. H. and Ohtori, Y., 1998, "Loading Rate of High Damping Seismic Isolation Rubber Bearing on Earthquake Responses," *KSME Int. J.*, Vol. 12, No. 1, pp. 58~66.
- Koo, G. H., Lee, J. H., Lee, H. Y. and Yoo, B., 1999, "Stability of Laminated Rubber Bearing and Its Application to Seismic Isolation," *KSME Int. J.*, Vol. 13, No. 8, pp. 595~604.
- Moon, B. Y., Kang, G. J., Kang, B. S. and Kim, K. S., 2002, "An Experimental Study on Fiber Reinforced Elastomeric Bearing," *Earthquake Engineering Society of Korea*, Vol. 6, No. 1, pp. 1~6.
- Moon, B. Y., Kang, G. J., Kang, B. S. and Kim, K. S., 2002, "Design and Experimental Analysis of Fiber Reinforced Elastomeric Isolator," *Transactions of the KSME. A.*, Vol. 26, No. 10, pp. 2026~2033.
- Tsai, H. C. and Lee, C. C., 1998, "Compressive Stiffness of Elastic Layers Bonded Between Rigid Plates," *International Journal of Solids and Structures*, Vol. 35, pp. 3053~3069.
- Tsai, H. C. and Lee, C. C., 1999, "Tilting Stiffness of Elastic Layers Bonded Between Rigid Plates," *International Journal of Solids and Structures*, Vol. 36, pp. 2485~2505.